Published in final edited form as:
Dev Biol. 2009 May 15; 329(2): 400–409. doi:10.1016/j.ydbio.2009.02.023.

Cyclical expression of the Notch/Wnt regulator Nrarp requires modulation by Dll3 in somitogenesis

William Sewell[1,†], **Duncan B. Sparrow**[2,3,†], **Allanceson J. Smith**[1], **Dorian M. Gonzalez**[4], **Eric F. Rappaport**[4], **Sally L. Dunwoodie**[2,3,5], and **Kenro Kusumi**[1,4,6,‡]

1 *School of Life Sciences, Arizona State University, Tempe, AZ 85287, USA*

2 *Victor Chang Cardiac Research Institute, Sydney, NSW 2010, Australia*

3 *St Vincent's Clinical School, Faculty of Medicine, University of New South Wales, NSW 2052, Australia*

4 *The Children's Hospital of Philadelphia, Philadelphia, PA 19104, USA*

5 *School of Biotechnology and Biomolecular Sciences, Faculty of Science, University of New South Wales, NSW 2052, Australia*

6 *Dept. of Basic Medical Sciences, The University of Arizona College of Medicine–Phoenix in partnership with Arizona State University, Phoenix, AZ 85004, USA*

Abstract

Delta-like 3 (*Dll3*) is a divergent ligand and modulator of the Notch signaling pathway only identified so far in mammals. Null mutations of *Dll3* disrupt cycling expression of Notch targets *Hes1*, *Hes5*, and *Lfng*, but not of *Hes7*. Compared with *Dll1* or *Notch1*, the effects of *Dll3* mutations are less severe for gene expression in the presomitic mesoderm, yet severe segmentation phenotypes and vertebral defects result in both human and mouse. Reasoning that *Dll3* specifically disrupts key regulators of somite cycling, we carried out functional analysis to identify targets accounting for the segmental phenotype. Using microdissected embryonic tissue from somitic and presomitic mesodermal tissue, we identified new genes enriched in these tissues, including *Limch1*, *Rphn2*, and *A130022J15Rik.* Surprisingly, we only identified a small number of genes disrupted by the *Dll3* mutation. These include *Uncx*, a somite gene required for rib and vertebral patterning, and *Nrarp*, a regulator of Notch/Wnt signaling in zebrafish and a cycling gene in mouse. To determine the effects of *Dll3* mutation on *Nrarp*, we characterized the cycling expression of this gene from early (8.5 dpc) to late (10.5 dpc) somitogenesis. *Nrarp* displays a distinct pattern of cycling phases when compared to *Lfng* and *Axin2* (a Wnt pathway gene) at 9.5 dpc but appears to be in phase with *Lfng* by 10.5 dpc. *Nrarp* cycling appears to require *Dll3* but not *Lfng* modulation. In *Dll3* null embryos, *Nrarp* displayed static patterns. However, in *Lfng* null embryos, *Nrarp* appeared static at 8.5 dpc but resumed cycling expression by 9.5 and dynamic expression at 10.5 dpc stages. By contrast, in *Wnt3a* null embryos, *Nrarp* expression was completely absent in the presomitic mesoderm. Towards identifying the role of *Dll3* in regulating somitogenesis, *Nrarp* emerges as a potentially important regulator that requires *Dll3* but not *Lfng* for normal function.

‡Author for correspondence: Kenro Kusumi, PhD, School of Life Sciences, Arizona State University, PO Box 874501, Tempe, AZ 85287-4501, USA, Tel. 1.480.727.8993; FAX 1.480.965.6899, Email: E-mail: kenro@asu.edu.
†These authors contributed equally.

Keywords

Nrarp; *Dll3*; *Uncx*; *Axin2*; *Lfng*; *Limch1*; *Rphn2*; delta-like 3; Notch; Wnt; presomitic mesoderm; somitogenesis; phase; segmentation; oscillatory

Introduction

The vertebrate body is shaped from segmental units called somites, which are formed in a regular, repeated fashion during embryonic development. Somites are produced at the anterior end of the unsegmented presomitic mesoderm (PSM), where oscillatory waves of gene expression regulate prepatterning of these segmental units (reviewed in Dequéant and Pourquié, 2008; Kageyama et al., 2007; Kulesa et al., 2007). To date, many genes have been identified that demonstrate such oscillatory expression, including the Notch pathway genes *Lfng*, *Hes1*, *Hes5*, and *Hes7* and the Wnt pathway genes *Axin2*, *Nkd1*, *Dact1* and *Dkk1* (Aulehla et al., 2003; Bessho et al., 2001; Dequéant et al., 2006; Forsberg et al., 1998; Ishikawa et al., 2004; Jouve et al., 2000).

The Wnt pathway plays a key role in the presomitic mesoderm. Small, irregular somites have been observed in beta-catenin null embryos and lengthened presomitic mesoderm observed in beta-catenin gain-of-function mutants, suggesting that the Wnt pathway regulates somitogenesis by activating target genes such as *Dll1* and positioning boundary determination genes in the anterior presomitic mesoderm (Dunty et al., 2007; Hofmann et al., 2004). *Wnt3a* mutants disrupt the expression of a number of Notch pathway genes including *Lfng*, whereas the Wnt pathway gene *Axin2* has been observed to display cycling expression in the Notch pathway *Dll1* mutant (Aulehla et al., 2003). These observations and others have been used to support the view that the Wnt pathway is upstream of Notch signaling in the PSM.

During somitogenesis, Notch signaling has been proposed to be essential for one or more of the following functions; generation of oscillatory gene expression in PSM cells (Holley et al., 2002; Jouve et al., 2000; Morales et al., 2002), establishment of somite compartment polarity (Barrantes et al., 1999; Saga, 2007; Takahashi et al., 2000), and communication between neighboring cells to synchronize oscillations (Horikawa et al., 2006; Jiang et al., 2000; Özbudak and Lewis, 2008). Recently, pharmacological blockade of the Notch pathway in zebrafish exhibited somite defects only after long developmental delays, suggesting Notch signaling is essential for synchronizing oscillations of neighboring cells in the posterior PSM but not for somite border formation (Mara et al., 2007; Özbudak and Lewis, 2008). Furthermore, Feller et al (2008) suggested a similar role for the Notch pathway in the caudal PSM in mice as well as demonstrating a requirement for Notch signaling in somite compartmentalization and not border formation in the anterior PSM. In mouse, defects in Notch signaling disrupt somite segmentation and oscillatory expression of Notch pathway genes in the PSM (Bessho et al., 2001; Conlon et al., 1995; Evrard et al., 1998; Feller et al., 2008; Hrabě de Angelis et al., 1997; Kusumi et al., 1998, 2004;). In PSM S-1, i.e., somite minus one, the region from which the next somite will form (Pourquié and Tam, 2001), the transcription factor *Mesp2*, a direct target of Notch signaling, appears to regulate segmental border formation through activation of *Epha4* and rostral-caudal compartmentalization through *Uncx*/*Uncx4.1* (reviewed in Saga, 2007). However, the mechanisms by which Notch signaling directs expression of downstream genes necessary for paraxial mesoderm segmentation is still not well understood.

Notch signaling activity can be modified in a number of ways (reviewed in Bray, 2006). Two modifiers of Notch signaling, *Lfng* and *Dll3*, are noteworthy given their disruption in humans causes a severe, autosomal recessive vertebral disorder, spondylocostal dysostosis (SCD;

Bulman et al., 2000; Sparrow et al., 2006). Disruptions of *Lfng* and *Dll3* in the mouse result in somitic and vertebral phenotypes that are morphologically similar to each other and to SCD (reviewed in Turnpenny et al., 2007). *Lfng* is a modifier of Notch signaling. It encodes a glycosyltransferase that modifies Notch in the Golgi, and modulates the ability of Notch to bind to DSL ligands. Loss of *Lfng* function results in severe rostrocaudal patterning defects (Evrard et al., 1998; Shifley et al., 2008; Zhang and Gridley, 1998). In contrast to *Lfng*, *Dll3* has only recently been identified as a modifier of Notch activity (Geffers et al., 2007). *Dll3* encodes a highly divergent delta-type DSL ligand that, unlike the other DSL ligands, does not appear to bind Notch receptors at the cell surface, and instead regulates Notch signaling, perhaps within the Golgi (Dunwoodie et al., 1997; Geffers et al., 2007; Ladi et al., 2005). Null alleles of *Dll3* disrupt transcriptional oscillation of some Notch pathway genes expressed in the PSM, as well as genes involved in determining the rostrocaudal polarity of the somite (Dunwoodie et al., 2002; Kusumi et al., 1998, 2004).

Loss of Notch signaling can lead to failure of Notch pathway gene expression during somitogenesis, as demonstrated in *Dll1* mutations which lead to severely decreased expression of most reported Notch pathway genes (Barrantes et al., 1999; Kusumi et al., 2004). By contrast, loss of *Dll3* results in decreased levels of gene expression of only some Notch pathway genes including *Hes5* and *Hes1*; but the dynamic expression of the cycling gene *Hes7* is unaffected (Dunwoodie et al., 2002; Kusumi et al., 2004). *Dll3* mutations also lead to the loss of *Lfng* cycling expression (Kusumi et al., 2004) and disruption of cycling patterns of activated Notch1 (Geffers et al., 2007). For comparison, loss of *Lfng* expression (Morimoto et al., 2005) or its cyclical component (Shifley et al., 2008) both disrupt cyclical activation of Notch1 and *Hes7* expression. In both humans and mice, *DLL3* mutations produce vertebral disruptions as severe as those observed in disruptions of *LFNG* or *HES7* (Bessho et al., 2001; Bulman et al., 2000; Dunwoodie et al., 2002; Kusumi et al., 1998; Sparrow et al., 2006, 2008).

Why does loss of *Dll3* produce such a severe phenotype? One possibility is that the disruptions in *Lfng* cycling expression and activated Notch1 patterns account for the severe phenotype. An alternate possibility is that as yet unidentified genes are critically required for somitogenesis, and that these are disrupted in *Dll3* mutants. Analysis of *Dll3* mutant embryos by microarray studies could identify such factors. Our understanding of somitogenesis continues to be advanced by the identification of new genes. This includes genes that are highly expressed in the presomitic mesoderm, as well as genes that have altered expression in segmental mutants. Functional genomic approaches can be particularly useful to find such genes, since they can screen the transcriptome, and microarray studies have identified genes with oscillatory expression in mouse somitogenesis (Dequéant et al., 2006) and in cell culture models of this process (William et al., 2007). Others have used this approach to examine *Dll1* (Machka et al (2005) and *Hes7* (Niwa et al. (2007) mutant embryos. Previously we reported expression differences in whole 9.5 dpc *Notch1* and *Dll3* mutant embryos (Loomes et al., 2007). However we did not identify somitogenesis genes, probably because the PSM is only a minor portion of the entire embryo. Here, we aimed to identify genes enriched in the presomitic mesoderm, and we have identified and characterized 3 genes expressed in the caudal PSM. In addition, we examined *Dll3* mutant PSM and somite level tissues, and identified a limited number of genes with disrupted expression. *Nrarp* (Notch regulated ankyrin repeat protein), which is normally expressed in a cycling manner during somitogenesis, emerged from our investigation as a gene that may contribute to the severe *Dll3* mutant phenotype.

Materials and Methods

Generation of mutant mice

Dll3^{tm1Rbe} (referred to as *Dll3*^{neo}), *Lfng*^{tm1Rjo}, and *Wnt3a*^{tm1Amc} mutations were crossed into the C57BL/6J background by backcross matings for over 10 generations (Dunwoodie et al., 2002; Kusumi et al., 1998; Takada et al., 1994). All animals were maintained according to Institutional Animal Care and Use Committee guidelines. *Dll3* mutants were generated by an intercross mating of $Dll3^{neo/+}$ mice, *Lfng* mutants were generated by an intercross mating of $Lfng^{tm1Rjo/+}$ mice, and *Wnt3a* mutants were produced by an intercross mating of $Wnt3a^{tm1Amc/+}$ mice. Genotypes for $Dll3^{neo}$, $Lfng^{tm1Rjo}$ and $Wnt3a^{tm1Amc}$ were determined by PCR assay as described previously (Dunwoodie et al., 2002; Evrard et al., 1997; Kusumi et al., 1998).

Microarray analysis

Embryos were collected at day 9.5 of gestation, and dissected from decidua in cold M2 medium (Nagy et al., 2003) containing 10% fetal calf serum. All remnants of the allantois were carefully removed from intact embryos, which were then cut at the boundary of the PSM and most recently-formed somite. The released tissue ("PSM level" containing tissue from all three germ layers) was placed in cold RNA lysis solution and frozen at −80°C for later RNA extraction. The remainder of the embryo was cut at the level of the otic placode, and the heart and endodermal tissues removed to generate the "somite level" samples. Total RNA was extracted from 9.5 dpc embryos using a SuperScript RT II Kit (Invitrogen) and subsequently used to synthesize double stranded cDNA. Biotinylated cRNA targets were prepared with a Bioarray HighYield RNA Transcript Labeling Kit (ENZO). Targets were hybridized to the Affymetrix MOE430A array according to manufacturer's protocol. Arrays were subsequently scanned using the following parameters: $t = 0.015$, $a_1 = 0.05$, $a_2 = 0.065$, median intensity value = 150. CEL files were normalized by the Robust Multichip Average method in order to compare the levels of expression between different samples and minimize technical variation accompanying use of the Genespring GX 7.3.2 module (Agilent).

Quantitative PCR

Quantitative PCR was used to confirm the expression of selected candidate genes, using cDNAs assayed by Taqman® Gene Expression Assays (Applied Biosystems). *Gapdh* was used to normalize Q-PCR results, using assay Mm99999915_g1. Assays for selected genes examined were: *Dll3* exons 2–3, Mm00432856_g1; *Dll3* exons 5–6, Mm00432853_g1; *Nrarp*, Mm00482529_s1; *Bcat2*, Mm00802196_g1; and *Hnrnpl*, Mm01172981_g1. Cycling conditions used for the Taqman Real-time PCR were: 95°C 10 minutes followed by 40 cycles of 95°C 15 seconds and 60°C 1 minute. Statistical analysis on expression data was carried out using a t-Test (two sample assuming unequal variance), with a threshold of $p<0.05$ on a two-tailed test on microarray data and at least a one-tailed test for validation by Q-PCR.

In situ hybridization

Whole mount *in situ* hybridizations were performed on 8.5, 9.5 and 10.5 dpc embryos as described previously (Harrison et al., 1995; Wilkinson, 1992). DNA templates for RNA probes were generated by RT-PCR from a 9.5 dpc embryo cDNA template. In brief, chimeric PCR templates were generated using 3′ end primers with the T7 RNA polymerase-binding site added. Digoxigenin-UTP labeled (Roche) RNA probes were generated by *in vitro* transcription (MAXIscript™, Ambion). RNA probes were purified using MC Free filtration units (Millipore). To compare the expression of two genes within the PSM, we bisected the caudal paraxial mesoderm of fixed whole 9.5 dpc embryos prior to *in situ* hybridization. Hybridized embryos were photographed using a SMZ1000 stereodissecting microscope (Nikon) with a Retiga CCD digital camera (Q-Imaging).

To examine cycling gene expression, we bisected the caudal paraxial mesoderm of 9.5 dpc embryos into axial halves, fixing one half in 4% paraformaldehyde while culturing the remaining half for 60, 120 or 180 min. in DMEM/50% FBS prior to fixation (adapted from Forsberg et al., 1998; Kusumi et al., 2004).

Accession numbers

Data sets from Affymetrix microarray analysis of microdissected embryonic tissues (MOE430A) are deposited at the Gene Expression Omnibus (www.ncbi.nlm.nih.gov/geo) with accession numbers (to be submitted before publication).

Results and Discussion

Microarray analysis of PSM and somite tissues

In carrying out microarray analysis of 9.5 dpc embryonic PSM and somite level tissues, we sought to 1.) identify genes that are enriched in PSM and somite tissues, and 2.) identify genes that were up- and down-regulated due to *Dll3* mutation. We microdissected tissue from 9.5 dpc embryos to generate somite and PSM level samples (Fig. 1A). Since the amount of tissue collected from the PSM of one embryo was insufficient for microarray analysis using a single round of target amplification, we pooled dissected samples from ten embryos. We sought to avoid double amplification protocols that can lead to distortion of gene expression levels. Microarray analysis using Affymetrix MOE430A arrays was carried out on the biological pool triplicates, and genes with greater than two-fold differences were identified (Supplemental Tables S1 and S2).

Expression analysis identified 66 genes with greater than two-fold increased expression in somite when compared to PSM fractions. Using the Gene Expression Database (GXD; http://www.informatics.jax.org/expression.shtml) and the published literature, we identified 15 genes that have been reported to be expressed in somites, including *Hes5*, *Meox1*, *Meox2*, *Pax1*, *Uncx*/*Uncx4.1*, and *Zic1* (Fig. 1B and Supplemental Table S1). We found a further 48 genes that were reported to be expressed in the other embryonic tissues, including the neural tube, surface ectoderm, or endoderm. Expression in the somites was not reported for these 48 genes and remains to be further characterized. Finally, there are also 3 genes whose expression has not been reported in embryos. We characterized the expression of these genes by *in situ* hybridization and observed that *Pkdcc* (protein kinase domain containing, cytoplasmic) was expressed in the endoderm, *Elavl4* (embryonic lethal abnormal vision-like 4) demonstrated a salt-and-pepper expression in the neuroepithelium of the midbrain and patches of expression dorsal to the second pharyngeal arch (data not shown), and *Itih5* (inter-alpha globulin inhibitor H5) expression was not detectable (Table 1 and Supplemental Fig. S1).

Identification of Limch1, and Rhpn2, and A130022J15Rik as novel genes expressed in the presomitic mesoderm

We further identified 87 genes with increased expression (≥ 2 fold) in the nascent PSM when compared to somite fractions (Figure 1C and Supplemental Table S2). As described above, we confirmed that 48 of these genes had been published as being expressed in PSM, including the somitogenesis genes *Dll1, Dll3, Fgf8, Hes7,* and *Tbx6*. 31 of these genes were reported to be expressed in the embryo in tissues including neural plate or surface ectoderm, but remain to be further examined in the paraxial mesoderm. This list includes the gene *Phlda2*, which interestingly is a paralogue of the Fas pathway gene *Phlda1* that cycles in phase with Wnt pathway genes (Dequéant et al., 2006). Finally, there are 8 genes whose expression has not been described in embryos (Table 1). We characterized these genes by *in situ* hybridization and noted high levels of PSM expression of three of them, *Limch1* (LIM & calponin homology domains 1), *Rhpn2* (rhophilin 2), and the cDNA *A130022J15Rik* (Fig. 1D–I). Gene Ontogeny predicts that *Limch1* encodes an actin binding protein and that *A130022J15Rik* encodes a glycosyltransferase, like *Lfng* (www.informatics.jax.org). Interestingly, *Rhpn2* encodes a rho GTPase binding protein that could play a role in endocytosis (Behrends et al., 2005). Endocytosis of Notch1 extracellular domain-ligand heterodimers and of Notch1 receptors play a key role in trans- and cis-regulation, respectively. A targeted mutation of *Rhpn2* has been generated and does not report any segmental defects, but the mutant was generated to examine thyroid function and segmentation may not have been examined in detail (Behrends et al., 2005). Targeted mutations or human mutations of *Limch1* and *A130022J15Rik* have not been reported. Another cDNA, *2610528A11Rik* was found to be localized to the caudal endoderm (Supplemental Fig. S1).

Dll3 mutation disrupts expression of the Notch regulator gene Nrarp

To enrich for genes in the paraxial mesoderm that are specifically disrupted by *Dll3* mutation, we compared microdissected tissues from wild-type and *Dll3* embryos. We generated biological replicate pools from *Dll3*$^{+/+}$ (wild-type) or *Dll3*$^{neo/neo}$ embryos for a total of twelve pools. Microarray analysis using Affymetrix MOE430A arrays was carried out on the biological pool triplicates, and genes with significant differences of greater than two-fold were selected. Findings were validated by Q-PCR and all expression differences were confirmed as statistically significant. *Dll3* itself displayed 3.6 fold decreased expression *Dll3*$^{neo/neo}$ embryos (Fig. 2A). This demonstrates that our microarray approach was capable of detecting relevant differences in gene expression between wild-type and null mutant embryos. A complete absence of *Dll3* transcripts might be expected in the *Dll3* null pools, and the Affymetrix probe set 1449236_at comprises oligonucleotides distributed over all of the *Dll3* exons, including exons 1–4 that were not removed in the targeted mutation (Netaffyx, www.affymetrix.com; Dunwoodie et al., 2002). We therefore used quantitative PCR to examine expression levels of *Dll3* exons 2–3 (not targeted) and exons 5–6 (deleted in the mutant; Fig. 2A). As expected, neither were detectable in *Dll3*$^{neo/neo}$ embryos, indicating that the targeted transcript was likely to have been subject to nonsense-mediated decay. Thus, levels of *Dll3* detected by microarray in *Dll3*$^{neo/neo}$ mutants appear to represent baseline noise of the microarray system.

Surprisingly, few other genes were identified at an initial 2-fold cut-off level. We next examined a group of genes identified at a threshold of 1.5 fold changes (Fig. 2). In addition to *Dll3*, only *Nrarp*, which has been previously identified as an inhibitor of the Notch signaling pathway, was downregulated in the *Dll3*$^{neo/neo}$ PSM fractions. *Nrarp* will be described in detail below. The only upregulated genes in these fractions were *Bcat2* (Fig. 2C), which encodes mitochondrial branched chain aminotransferase 2 that produces a growth and metabolic defect when knocked out (She et al., 2007) and *Hnrnpl* (Fig. 2D, E), which encodes heterogeneous nuclear riboprotein L factor that plays a role in mRNA processing (Griffith et al., 2006). We found that *Bcat2* is highly expressed in the rostral first pharyngeal arch and also expressed in trunk mesenchyme and that *Hnrnpl* is expressed ubiquitously at 9.5 dpc (Supplemental Fig. S1). Since mRNA splicing is a key regulatory step for the dynamically expressed Notch pathway cycling genes, the upregulation of *Hnrnpl* may represent a compensatory change in response to disruption of the segmentation clock. However, the altered expression of both of these genes may be secondary to the disruption in Notch signaling.

In tissue collected from somite levels, *Hnrnpl* was the only gene that displayed increased expression in *Dll3* mutants, and given the ubiquitous expression that we observed at 9.5 dpc, this is not surprising. We found that *Uncx*/*Uncx4.1* was decreased in expression (Fig. 2E). *Uncx* is expressed in the caudal compartment of somites, and we have previously shown that *Dll3* mutant embryos display disrupted expression in rostral-caudal compartments of somites (Dunwoodie et al., 2002). *Uncx* expression is also severely down-regulated in *Dll1* and *RBPjk* null embryos when Notch1 signaling is absent (Barrantes et al., 1999;Takahashi et al., 2003). *Uncx* is required for the formation of the pedicles and proximal ribs, structures which are malformed in *Dll3* mutant animals (Kusumi et al., 1998;Mansouri et al., 2000). However, the vertebral malformations in *Uncx* mutants are distinct from those observed in *Dll3* and much less severe. Therefore, the malformations observed due to *Dll3* mutation are not likely to be mostly accounted for by *Uncx*-mediated effects.

The Notch pathway gene Nrarp displays cycling expression during somitogenesis

Evidence suggests that *Nrarp* may regulate both the Notch and Wnt signaling pathways. *Nrarp* was originally identified in an expression screen in *Xenopus* embryos as a member of the Delta-Notch pathway (Gawantka et al., 1998). In *Xenopus*, activation of the Notch pathway resulted in elevated levels of *Nrarp* expression, demonstrating *Nrarp* is a target of the Notch pathway (Lamar et al., 2001). Once expressed, *Nrarp* functions as a negative feedback regulator of Notch signaling by binding the activated form of Notch (Notch-ICD) and promoting a decrease in Notch-ICD levels and a reduction in Notch target gene expression. *Nrarp* has also been found to be a positive regulator of the Wnt pathway in zebrafish, by stabilizing the LEF1 protein (Ishitani et al., 2005). Furthermore, the activation of LEF1 was not found to affect Notch signaling in zebrafish, so the actions of *Nrarp* appear to act independently on the canonical Wnt and Notch signaling pathways.

In the mouse, *Nrarp* was described as being expressed within the paraxial mesodermal in a rostral band and a broad caudal domain in the PSM; however, in this study *Nrarp* was not noted as a cycling gene (Krebs et al., 2001). The rostral band was localized to the caudal S0 (the newly forming somite). The broad caudal domain of *Nrarp* in the PSM was defined by a rostral boundary at the second presumptive somite (S-2). These were spatially verified by comparison with *Uncx*, a marker for the somite caudal compartment, and *Mesp2*, a marker for the anterior half of the second presumptive somite in the PSM (Krebs et al., 2001). More recently, *Nrarp* was described to display cycling expression based on identification in a microarray-based screen for genes with oscillatory expression in mouse PSM (Dequéant et al., 2006); and two expression phases for *Nrarp* have been described (Dequéant et al., 2006, Shifley et al., 2008).

While *Nrarp* expression in PSM has been reported at particularly stages, we sought to fully characterize the cycling expression of *Nrarp* in the PSM from early to late-somitogenesis at 8.5, 9.5, and 10.5 dpc. First we identified that distinct caudal-to-rostral shifts, characteristic of cycling genes, occurred at each stage (Fig. 3). Rostral bands of *Nrarp* expression displayed anterograde shifts and rostrocaudal contraction characteristic of cycling genes at all three stages. At 8.5 and 9.5 dpc, *Nrarp* expression in the caudal PSM extended over a large proportion of the PSM, but the most intense areas of expression displayed anterograde shifts. In addition, there was strong expression of *Nrarp* remaining in the primitive streak in 8.5 dpc embryos, similar to other Notch pathway genes such as *Lfng* (Barrantes et al., 1999;Dunwoodie et al., 1997). At 9.5 dpc, there was a residual level of *Nrarp* expression remaining throughout the PSM. At 10.5 dpc, cycling patterns of *Nrarp* caudal bands were more clearly evident due to loss of this residual expression in the PSM and the tailbud.

The phase of a cycling gene is defined by its spatial expression along the caudal-to-rostral axis within the embryonic PSM at a particular point in time during a segmentation cycle (Pourquié and Tam, 2001). Using the phase descriptions used for other cycling genes, we defined three phases for *Nrarp* expression (Fig. 3G–I and M–O). In phase I, caudal expression of *Nrarp* remained in S1 at 8.5 and 9.5 dpc, but not at 10.5 dpc. Rostral bands of *Nrarp* expression in S0/S1 contracted along the rostrocaudal axis between phase I and III. Expression of *Nrarp* in the PSM was localized to the tailbud and caudal region in phase I, shifted rostrally in phase II, and condensed towards S-2 in phase III. Thorough description of these phases was a necessary step prior to analysis of effects of *Dll3*, *Lfng*, and *Wnt3a* mutations on *Nrarp* cycling expression.

Nrarp cycling expression displays a 2 hour periodicity

Mouse embryos were bisected at 9.5 dpc, with left halves cultured for 15 minutes and then fixed, and right halves cultured for an additional 1 hour (Fig. 4A, n=8), 2 hours (Fig. 4B, n=7), or 3 hours (Fig. 4C, n=7) prior to fixation. Culturing led to a slight contraction of embryonic explant tissues, therefore halves were aligned with the first morphologically apparent forming somite. At a 1 hour time difference, anterograde shifts of *Nrarp* caudal expression were observed (Fig. 4A). At a 2 hour time difference, cultured halves displayed similar expression patterns of *Nrarp*, as shown in (Fig. 4B). At 3 hour time differences, cultured halves again differed in *Nrarp* caudal expression (Fig. 4C). The observation that cultured halves were in the same phase at 2 hours and out of phase at 1 and 3 hours is consistent with the 2 hour periodicity of cycling genes during mouse somitogenesis (Hirata et al., 2002).

Nrarp cycling phases relative to Lfng and the Wnt pathway gene Axin2 at 9.5 and 10.5 dpc

Cycling genes tend to fall into two classes – those which cycle in concert with Notch and FGF pathway genes, and Wnt pathway-associated genes that do not. Comparing expression patterns of cycling genes can help give clues about the dynamics within and between gene pathways. Genes have been described as being “in phase” if similar expression patterns from phase I to III are observed for the two genes. Previous models have proposed that cycling genes within the same pathway will display more similar phases than genes in different pathways (Aulehla et al., 2003; Dequéant and Pourquié, 2008). When assayed by microarray analysis of caudal PSM tissues, levels of *Nrarp* expression were shown to peak in correlation with *Lfng* but not with *Axin2* (Dequéant et al., 2006). Some genes such as *Nkd1* have been shown to display dependency on both Notch and Wnt signaling, with *Nkd1* transcription requiring *Wnt3a* and Notch signaling for oscillatory expression (Ishikawa et al., 2004).

We used bisected embryos to directly compare *Nrarp* cycling phases I, II, and III with patterns for *Lfng* and *Axin2* in the other half (Fig. 5). We observed that the caudal-to-rostral progression and boundaries of *Nrarp* within the PSM were more comparable to that of the Notch modulator *Lfng* at 10.5 dpc (Fig. 5A–C; phases for *Nrarp* as diagrammed in Fig. 2) than at 9.5 dpc (Supplemental Fig. S2, A–C). In comparison, *Nrarp* patterns were distinct from the caudal-to-rostral progression of *Axin2* at 10.5 dpc (Fig. 5D–F) and 9.5 dpc (Supplemental Fig. S2, D–F). Previous reports have described *Lfng* and *Axin2* expression as being out of phase with each other (Aulehla et al., 2003), and we also observed out of phase patterns at 10.5 dpc (Fig. 5G–I). In contrast, the phase differences between *Lfng* and *Axin2* were more difficult to detect at 9.5 dpc, suggesting that these genes may grow increasingly out of phase as somitogenesis progresses (Supplemental Fig. S2 G–I, n=9).

To further investigate these observations, we categorized 9.5 and 10.5 dpc embryos that were probed for *Nrarp, Lfng* and *Axin2* (Table 2). Expression phases I, II, and III have often been envisioned as consisting of equal representation of embryos during cycling, and by inference, relatively equal time periods. We observed for *Lfng* and *Axin2*, that departure from equal distribution between phases I–III was not significant by X^2 analysis (Table 2). In contrast, *Nrarp* expression departed significantly from equal distribution between the three phases. For *Nrarp* expression at 9.5, this may be partially accounted for by the greater region of *Nrarp* expression along rostrocaudal PSM axis (Fig. 3), but this effect is also observed for *Nrarp* at 10.5 dpc. Therefore, the assumption that the amount of time that cycling genes spend in phases I, II, or III may not be equal for all genes. It is possible that *Nrarp* “rushes” through phase III, making it less likely to be represented.

Nrarp requires Lfng early in somitogenesis but requires Dll3 to maintain cycling expression

Given that our microarray analysis of *Dll3^neo^* null embryos identified *Nrarp* as one of a limited number of genes with decreased expression, we examined the spatiotemporal pattern of *Nrarp* by whole mount *in situ* hybridization. In 9.5 dpc *Dll3^neo^* homozygous embryos, *Nrarp* expression appeared to be fixed in phase I (n=9; Fig. 6A), and by 10.5 dpc, *Nrarp* showed decreased expression in the caudal PSM and in the newly forming somite, S0 (Fig. 6E). *Nrarp* cycling expression was observed in *Dll3^neo^* heterozygous embryos (Fig. 6B–D, F–H) and wild-type embryos (data not shown). The static pattern of *Nrarp* expression in *Dll3* null mutants fixed in phase I bares a strong resemblance to the static pattern of activated Notch1 expression in *Dll3* null mutants at 10.5 dpc (Geffers et al., 2007). Static patterns of activated Notch1 expression have also been observed in *Lfng* null mutants at 11.5 dpc (Morimoto et al., 2005). In *Dll3* mutants, the Notch pathway cycling genes *Hes1*, *Hes5*, and *Lfng* are also frozen in a single phase (Dunwoodie et al., 2002;Kusumi et al., 2004). Interestingly, only *Hes7* manages to maintain oscillation in *Dll3* null embryos, in contrast to findings in embryos constitutively expressing Notch1-ICD (Feller et al., 2008), suggesting that the autoregulatory feedback loop for this bHLH factor is less dependent on Notch signaling to cycle (Kusumi et al., 2004).

To compare the effects of mutations in *Lfng* with those in *Dll3* on *Nrarp* cycling expression, we examined *Lfng* mutant embryos at 9.5 dpc. We observed that *Nrarp* expression appeared to be cycling in $Lfng^{tm1Rjo}$ null mutants at 9.5 dpc (Fig. 7E–G) and dynamic in the caudal PSM at 10.5 dpc (Fig. 7K–M) without the characteristic caudal-to-rostral "wave" seen in wild-type embryos (Fig. 7N–P). *Nrarp* expression did not appear to be highly dynamic early in somitogenesis at 8.5 dpc (Fig. 7A–B). It is interesting that, despite reports that activated Notch1 does not cycle in *Lfng* null mutants at 11.5 dpc (Morimoto et al., 2005), *Nrarp* appears to somehow be "kick-started" to display cycling expression later in somitogenesis. In contrast, *Nrarp* does not cycle in *Dll3* mutants, thus suggesting that factors in addition to activated Notch1 cycling are required for somitogenesis.

Nrarp has been reported to display stable expression at 8.5 dpc in *Lfng* mutants with a specific disruption of a regulatory element required for oscillatory expression (Shifley et al., 2008). However, by 10.5 dpc in embryos lacking cycling *Lfng*, *Nrarp* cycling recovers (Shifley et al., 2008). Before *Nrarp* was reported to display cycling expression, the effects of *Notch1*, *Dll1*, *Lfng* and $Dll3^{pu}$ mutations on *Nrarp* expression had been described for the paraxial mesoderm (Krebs et al., 2001). Both *Notch1* and *Dll1* null mutants result in severe down-regulation of *Nrarp* in the PSM. Thus, the *Dll1* and *Dll3* ligands have very different effects on *Nrarp* expression. Differential functions for delta proteins and splice variants have also been described in zebrafish (Mara et al., 2007, 2008). *Nrarp* expression in null *Lfng* embryos was reported to be severely down-regulated for rostral PSM but not caudal PSM expression. This does not agree with the findings of Shifley et al (2008) and our observations; however, this observation was made before *Nrarp* was known to be a cycling gene and may be describing different normal phases.

Nrarp expression is not observed in Wnt3a mutants

Wnt signaling is required for the expression of many Notch and Wnt pathway genes in the PSM (Aulehla et al., 2003, 2008). Wnt signaling acts to restrict boundary determination genes to the anterior PSM where somite size, morphology and polarity are defined (Dunty et al., 2008). Genes in other pathways such as *Cdx2* and *Cdx4* do not require *Wnt3a* for expression within the PSM (Ikeya and Takada, 2001). Given the role of Wnt signaling in regulating PSM formation and maintenance, we examined *Nrarp* expression in mutants disrupted for Wnt signaling ($Wnt3a^{tm1Amc}$ mutants; Fig. 8). $Wnt3a^{tm1Amc/tm1Amc}$ embryos lack caudal somites and a tail bud and exhibit axial truncation (Takada et al., 1994). At 8.5 dpc, $Wnt3a^{tm1Amc/tm1Amc}$ embryos expressed *Cdx4* at comparable levels to +/+ (Fig. 8D, E), suggesting the presence of paraxial and lateral mesoderm. However, *Nrarp* expression was severely down-regulated (Fig. 8A), compared to heterozygous and +/+ embryos (Fig. 8B–C). At 9.5 dpc, $Wnt3a^{tm1Amc/tm1Amc}$ embryos exhibited severely malformed and decreased amounts of PSM, confirmed by *Cdx4* hybridization (Fig. 8I), and the remaining tissue also did not show any expression of *Nrarp* (Fig. 8F), compared to wild-type controls (Fig. 8G–H). Thus, it appears that *Nrarp* requires Wnt signaling to initiate expression within the PSM.

Developmental functions of Nrarp

There are two paralogues of *Nrarp* in the zebrafish. Morpholino-based knockdown of *Nrarp-a* expression in zebrafish has been reported to result in slightly smaller animals with altered pigmentation and curly and shortened tail phenotypes (Ishitani et al., 2005). These phenotypes likely result from the destabilization of LEF1 protein by removing the ubiquitylation-blocking function of Nrarp, resulting in altered neural crest development. The shortened tail phenotype does not appear to be due to major disruptions in somite patterning, but more subtle malformations remain possible (M. Itoh, personal communication). In contrast, *Nrarp-b* morphants did not display any phenotype. However, knockdown of *Nrarp-a* and *–b* enhanced expression of *her1* indicating they function redundantly as negative regulators of Notch signaling during somitogenesis in zebrafish (Ishitani et al., 2005). The phenotypes of *Nrarp a*/*b* morphants were not described, therefore, the presence of two *Nrarp* homologues raises the possible that overlapping function that might make it difficult to detect vertebral phenotypes.

To date, there are no reports of targeted mutations in the mouse or human genetic disorders associated with *NRARP* alleles. However, the lack of a segmentation phenotype in a targeted mutation of *Nrarp* alone would not necessarily eliminate a role in somitogenesis. Knockouts of the cycling genes *Hes1* and *Axin2* do not have any reported somite phenotypes, despite their key roles in the segmentation regulatory mechanism (Ishibashi et al., 1995; Lustig et al., 2002; Tomita et al., 1996). Within the Notch pathway, overlapping function of homologues can make phenotypes difficult to examine in single gene mutations, e.g., *Mfng* and *Rfng* mutations do not have an observable phenotype but display liver phenotypes when crossed with mutations in the paralogous gene *Lfng* (Ryan et al., 2008). Paralogues of *Nrarp* have not been described in either the mouse or human genomes.

Downstream effects of DLL3 mutation and vertebral phenotypes

Human mutations in *DLL3* have been identified in spondylocostal dysostosis type I (SCD1), which has been distinguishable by radiologists from SCD3 caused by mutations in *LFNG*, and more recently in SCD4 due to mutations in *HES7* (Bulman et al., 2000; Sparrow et al., 2006, 2008; Turnpenny et al., 2007). Mouse osteological changes have not been examined so far at comparable detail. With the observation that *Dll3* mutation leads to disruptions of *Uncx* and *Nrarp* expression, it is possible that the unique SCD1 phenotypes due to *DLL3* mutation may be accounted for by disruptions in regulation of these two genes. *Uncx* plays a key role in shaping the proximal ribs and the pedicles, the portions of the vertebrae that are between the vertebral body and the bilateral transverse processes (Mansouri et al., 2000). The *Dll3* pudgy and targeted mutation alleles both display proximal rib fusions and bifurcations, and dysregulation of *Uncx* may play a role in these anomalies. Identification of *Uncx* from these studies also warrants more careful examination of human and mouse pedicle osteology in mutants. As described above, *Nrarp* mutations in mouse or human have not yet been identified. Given its cycling expression in somitogenesis and identification as down-regulated in *Dll3* null mutants, information about the phenotype in *Nrarp* mutants would allow us to evaluate this gene in contributing to *DLL3*-related defects and as a candidate for human disorders of the spine.

Supplementary Material

Refer to Web version on PubMed Central for supplementary material.

Acknowledgments

We thank Joshua Gibson, Walter Eckalbar and Michael Chacon for technical assistance. We thank Stephen Pratt for helpful discussions. This work was supported by NIH RO1 AR050687 (KK) and a Hitchings-Elion Fellowship of the Burroughs Wellcome Fund (KK), National Health and Medical Research Council (NHMRC) Project Grant 404804

(SLD and DBS), a Westfield-Belconnen Fellowship (DBS), a Pfizer Foundation Australia Senior Research Fellowship (SLD) and a NHMRC Senior Research Fellowship (SLD).

References

Aulehla A, Wiegraebe W, Baubet V, Wahl MB, Deng C, Taketo M, Lewandoski M, Pourquié O. A beta-catenin gradient links the clock and wavefront systems in mouse embryo segmentation. Nat Cell Biol 2008;10:186–93. [PubMed: 18157121]

Aulehla A, Wehrle C, Brand-Saberi B, Kemler R, Gossler A, Kanzler B, Herrmann BG. *Wnt3a* plays a major role in the segmentation clock controlling somitogenesis. Dev Cell 2003;4:395–406. [PubMed: 12636920]

Barrantes, IdB; Elia, AJ.; Wünsch, K.; Hrabě De Angelis, M.; Mak, TW.; Rossant, J.; Conlon, RA.; Gossler, A.; de la Pompa, JL. Interaction between Notch signalling and Lunatic fringe during somite boundary formation in the mouse. Curr Biol 1999;9:470–480. [PubMed: 10330372]

Behrends J, Clement S, Pajak B, Pohl V, Maenhaut C, Dumont JE, Schurmans S. Normal thyroid structure and function in rhophilin 2-deficient mice. Mol Cell Biol 2005;25:2846–2852. [PubMed: 15767687]

Bessho Y, Sakata R, Komatsu S, Shiota K, Yamada S, Kageyama R. Dynamic expression and essential functions of *Hes7* in somite segmentation. Genes Dev 2001;15:2642–2647. [PubMed: 11641270]

Bray SJ. Notch signalling: a simple pathway becomes complex. Nat Rev Mol Cell Biol 2006;7:678–89. [PubMed: 16921404]

Bulman MP, Kusumi K, Frayling TM, McKeown C, Garrett C, Lander ES, Krumlauf R, Hattersley AT, Ellard S, Turnpenny PD. Mutations in the human delta homologue, DLL3, cause axial skeletal defects in spondylocostal dysostosis. Nat Genet 2000;24:438–441. [PubMed: 10742114]

Conlon RA, et al. Notch1 is required for the coordinate segmentation of somites. Development 1995;121:1533–45. [PubMed: 7789282]

Dequéant ML, Glynn E, Gaudenz K, Wahl M, Chen J, Mushegian A, Pourquié O. A complex oscillating network of signaling genes underlies the mouse segmentation clock. Science 2006;314:1595–1598. [PubMed: 17095659]

Dequéant ML, Pourquié O. Segmental patterning of the vertebrate embryonic axis. Nat Rev Genet 2008;9:370–82. [PubMed: 18414404]

Dunty WC Jr, Biris KK, Chalamalasetty RB, Taketo MM, Lewandoski M, Yamaguchi TP. Wnt3a/beta-catenin signaling controls posterior body development by coordinating mesoderm formation and segmentation. Development 2008;135:85–94. [PubMed: 18045842]

Dunwoodie SL, Henrique D, Harrison SM, Beddington RS. Mouse *Dll3*: a novel divergent Delta gene which may complement the function of other Delta homologues during early pattern formation in the mouse embryo. Development 1997;124:3065–3076. [PubMed: 9272948]

Dunwoodie SL, Clements M, Sparrow DB, Sa X, Conlon RA, Beddington RS. Axial skeletal defects caused by mutation in the spondylocostal dysplasia/pudgy gene *Dll3* are associated with disruption of the segmentation clock within the presomitic mesoderm. Development 2002;129:1795–1806. [PubMed: 11923214]

Evrard YA, et al. lunatic fringe is an essential mediator of somite segmentation and patterning. Nature 1998;394:377–81. [PubMed: 9690473]

Feller J, Schneider A, Schuster-Gossler K, Gossler A. Noncyclic Notch activity in the presomitic mesoderm demonstrates uncoupling of somite compartmentalization and boundary formation. Genes Dev 2008;22:2166–71. [PubMed: 18708576]

Forsberg H, Crozet F, Brown NA. Waves of mouse *Lunatic fringe* expression, in four-hour cycles at two-hour intervals, precede somite boundary formation. Curr Biol 1998;8:1027–1030. [PubMed: 9740806]

Gawantka V, Pollet N, Delius H, Vingron M, Pfister R, Nitsch R, Blumenstock C, Niehrs C. Gene expression screening in *Xenopus* identifies molecular pathways, predicts gene function and provides a global view of embryonic patterning. Mech Dev 1998;77:95–141. [PubMed: 9831640]

Geffers I, Serth K, Chapman G, Jaekel R, Schuster-Gossler K, Cordes R, Sparrow DB, Kremmer E, Dunwoodie SL, Klein T, Gossler A. Divergent functions and distinct localization of the Notch ligands DLL1 and DLL3 in vivo. J Cell Biol 2007;178:465–476. [PubMed: 17664336]

Griffith BN, Walsh CM, Szeszel-Fedorowicz W, Timperman AT, Salati LM. Identification of hnRNPs K, L and A2/B1 as candidate proteins involved in the nutritional regulation of mRNA splicing. Biochim Biophys Acta 2006;1759:552–561. [PubMed: 17095106]

Harrison SM, Dunwoodie SL, Arkell RM, Lehrach H, Beddington RS. Isolation of novel tissue-specific genes from cDNA libraries representing the individual tissue constituents of the gastrulating mouse embryo. Development 1995;121:2479–2489. [PubMed: 7671812]

Hirata H, Yoshiura S, Ohtsuka T, Bessho Y, Harada T, Yoshikawa K, Kageyama R. Oscillatory expression of the bHLH factor Hes1 regulated by a negative feedback loop. Science 2002;298:840–843. [PubMed: 12399594]

Hofmann M, Schuster-Gossler K, Watabe-Rudolph M, Aulehla A, Herrmann BG, Gossler A. WNT signaling, in synergy with T/TBX6, controls Notch signaling by regulating Dll1 expression in the presomitic mesoderm of mouse embryos. Genes Dev 2004;18:2712–2717. [PubMed: 15545628]

Holley SA, Jülich D, Rauch GJ, Geisler R, Nüsslein-Volhard C. *her1* and the *notch* pathway function within the oscillator mechanism that regulates zebrafish somitogenesis. Development 2002;129:1175–1183. [PubMed: 11874913]

Horikawa K, Ishimatsu K, Yoshimoto E, Kondo S, Takeda H. Noise-resistant and synchronized oscillation of the segmentation clock. Nature 2006;441:719–23. [PubMed: 16760970]

Hrabě de Angelis M, McIntyre J 2nd, Gossler A. Maintenance of somite borders in mice requires the Delta homologue *DII1*. Nature 1997;386:717–721. [PubMed: 9109488]

Ikeya M, Takada S. Wnt-3a is required for somite specification along the anteroposterior axis of the mouse embryo and for regulation of cdx-1 expression. Mech Dev 2001;103:27–33. [PubMed: 11335109]

Ishibashi M, Ang S-L, Shiota K, Nakanishi S, Kageyama R, Guillemot F. Targeted disruption of mammalian hairy and Enhancer of split homolog-1 (HES-1) leads to up-regulation of neural helix-loop-helix factors, premature neurogenesis, and severe neural tube defects. Genes Dev 1995;9:3136–3148. [PubMed: 8543157]

Ishikawa A, Kitajima S, Takahashi Y, Kokubo H, Kanno J, Inoue T, Saga Y. Mouse *Nkd1*, a Wnt antagonist, exhibits oscillatory gene expression in the PSM under the control of Notch signaling. Mech Dev 2004;121:1443–1453. [PubMed: 15511637]

Ishitani T, Matsumoto K, Chitnis AB, Itoh M. Nrarp functions to modulate neural-crest-cell differentiation by regulating LEF1 protein stability. Nat Cell Biol 2005;7:1106–1112. [PubMed: 16228014]

Jiang YJ, et al. Notch signalling and the synchronization of the somite segmentation clock. Nature 2000;408:475–9. [PubMed: 11100729]

Jouve C, Palmeirim I, Henrique D, Beckers J, Gossler A, Ish-Horowicz D, Pourquié O. Notch signalling is required for cyclic expression of the hairy-like gene *HES1* in the presomitic mesoderm. Development 2000;127:1421–1429. [PubMed: 10704388]

Kageyama R, Yoshiura S, Masamizu Y, Niwa Y. Ultradian oscillators in somite segmentation and other biological events. Cold Spring Harb Symp Quant Biol 2007;72:451–457. [PubMed: 18419304]

Krebs LT, Deftos ML, Bevan MJ, Gridley T. The *Nrarp* gene encodes an ankyrin-repeat protein that is transcriptionally regulated by the notch signaling pathway. Dev Biol 2001;238:110–119. [PubMed: 11783997]

Kulesa PM, Schnell S, Rudloff S, Baker RE, Maini PK. From segment to somite: segmentation to epithelialization analyzed within quantitative frameworks. Dev Dyn 2007;236:1392–402. [PubMed: 17497694]

Kusumi K, Sun ES, Kerrebrock AW, Bronson RT, Chi DC, Bulotsky MS, Spencer JB, Birren BW, Frankel WN, Lander ES. The mouse pudgy mutation disrupts Delta homologue *Dll3* and initiation of early somite boundaries. Nat Genet 1998;19:274–278. [PubMed: 9662403]

Kusumi K, Mimoto MS, Covello KL, Beddington RS, Krumlauf R, Dunwoodie SL. *Dll3* pudgy mutation differentially disrupts dynamic expression of somite genes. Genesis 2004;39:115–121. [PubMed: 15170697]

Ladi E, Nichols JT, Ge W, Miyamoto A, Yao C, Yang LT, Boulter J, Sun YE, Kintner C, Weinmaster G. The divergent DSL ligand Dll3 does not activate Notch signaling but cell autonomously attenuates signaling induced by other DSL ligands. J Cell Biol 2005;170:983–92. [PubMed: 16144902]

Lamar E, Deblandre G, Wettstein D, Gawantka V, Pollet N, Niehrs C, Kintner C. *Nrarp* is a novel intracellular component of the Notch signaling pathway. Genes Dev 2001;15:1885–1899. [PubMed: 11485984]

Loomes KM, Stevens SA, O'Brien ML, Gonzalez DM, Ryan MJ, Segalov M, Dormans NJ, Mimoto MS, Gibson JD, Sewell W, Schaffer AA, Nah HD, Rappaport EF, Pratt SC, Dunwoodie SL, Kusumi K. *Dll3* and *Notch1* genetic interactions model axial segmental and craniofacial malformations of human birth defects. Dev Dyn 2007;236:2943–2951. [PubMed: 17849441]

Lustig B, Jerchow B, Sachs M, Weiler S, Pietsch T, Karsten U, van de Wetering M, Clevers H, Schlag PM, Birchmeier W, Behrens J. Negative feedback loop of Wnt signaling through upregulation of conductin/axin2 in colorectal and liver tumors. Mol Cell Biol 2002;22:1184–1193. [PubMed: 11809809]

Machka C, Kersten M, Zobawa M, Harder A, Horsch M, Halder T, Lottspeich F, Hrabě de Angelis M, Beckers J. Identification of *Dll1* (Delta1) target genes during mouse embryogenesis using differential expression profiling. Gene Expr Patterns 2005;6:94–101. [PubMed: 15979417]

Mansouri A, Voss AK, Thomas T, Yokota Y, Gruss P. Uncx4.1 is required for the formation of the pedicles and proximal ribs and acts upstream of Pax9. Development 2000;127:2251–8. [PubMed: 10804168]

Mara A, Schroeder J, Chalouni C, Holley SA. Priming, initiation and synchronization of the segmentation clock by deltaD and deltaC. Nat Cell Biol 2007;9:523–530. [PubMed: 17417625]

Mara A, Schroeder J, Holley SA. Two deltaC splice-variants have distinct signaling abilities during somitogenesis and midline patterning. Dev Biol 2008;318:126–132. [PubMed: 18430417]

Morales AV, Yasuda Y, Ish-Horowicz D. Periodic Lunatic fringe expression is controlled during segmentation by a cyclic transcriptional enhancer responsive to notch signaling. Dev Cell 2002;3:63–74. [PubMed: 12110168]

Morimoto M, Takahashi Y, Endo M, Saga Y. The Mesp2 transcription factor establishes segmental borders by suppressing Notch activity. Nature 2005;435:354–9. [PubMed: 15902259]

Nagy, A.; Gertsenstein, M.; Vintersten, K.; Behringer, R. A Laboratory Manual. Cold Spring Harbor Laboratory Press; New York: 2003. Manipulating the Mouse Embryo.

Niwa Y, Masamizu Y, Liu T, Nakayama R, Deng CX, Kageyama R. The initiation and propagation of Hes7 oscillation are cooperatively regulated by Fgf and notch signaling in the somite segmentation clock. Dev Cell 2007;13:298–304. [PubMed: 17681139]

Özbudak EM, Lewis J. Notch signalling synchronizes the zebrafish segmentation clock but is not needed to create somite boundaries. PLoS Genet 2008;4:e15. [PubMed: 18248098]

Pourquié O, Tam PP. A nomenclature for prospective somites and phases of cyclic gene expression in the presomitic mesoderm. Dev Cell 2001;1:619–620. [PubMed: 11709182]

Ryan MJ, Bales C, Nelson A, Gonzalez DM, Underkoffler L, Segalov M, Wilson-Rawls J, Cole SE, Moran JL, Russo P, Spinner NB, Kusumi K, Loomes KM. Bile duct proliferation in Jag1/fringe heterozygous mice identifies candidate modifiers of the alagille syndrome hepatic phenotype. Hepatology 2008;48:1989–1997. [PubMed: 19026002]

Saga Y. Segmental border is defined by the key transcription factor Mesp2, by means of the suppression of Notch activity. Dev Dyn 2007;236:1450–5. [PubMed: 17394251]

She P, Reid TM, Bronson SK, Vary TC, Hajnal A, Lynch CJ, Hutson SM. Disruption of BCATm in mice leads to increased energy expenditure associated with the activation of a futile protein turnover cycle. Cell Metab 2007;6:181–194. [PubMed: 17767905]

Shifley ET, Vanhorn KM, Perez-Balaguer A, Franklin JD, Weinstein M, Cole SE. Oscillatory lunatic fringe activity is crucial for segmentation of the anterior but not posterior skeleton. Development 2008;135:899–908. [PubMed: 18234727]

Sparrow DB, et al. Mutation of the LUNATIC FRINGE gene in humans causes spondylocostal dysostosis with a severe vertebral phenotype. Am J Hum Genet 2006;78:28–37. [PubMed: 16385447]

Sparrow DB, Guillén-Navarro E, Fatkin D, Dunwoodie SL. Mutation of Hairy-and-Enhancer-of-Split-7 in humans causes spondylocostal dysostosis. Hum Mol Genet 2008;17:3761–3766. [PubMed: 18775957]

Takada S, Stark KL, Shea MJ, Vassileva G, McMahon JA, McMahon AP. *Wnt-3a* regulates somite and tailbud formation in the mouse embryo. Genes Dev 1994;8:174–189. [PubMed: 8299937]

Takahashi Y, et al. *Mesp2* initiates somite segmentation through the *Notch* signalling pathway. Nat Genet 2000;25:390–396. [PubMed: 10932180]

Takahashi Y, Inoue T, Gossler A, Saga Y. Feedback loops comprising Dll1, Dll3 and Mesp2, and differential involvement of Psen1 are essential for rostrocaudal patterning of somites. Development 2003;130:4259–4268. [PubMed: 12900443]

Tomita K, Ishibashi M, Nakahara K, Ang SL, Nakanishi S, Guillemot F, Kageyama R. Mammalian hairy and Enhancer of split homolog 1 regulates differentiation of retinal neurons and is essential for eye morphogenesis. Neuron 1996;16:723–734. [PubMed: 8607991]

Turnpenny PD, Alman B, Cornier AS, Giampietro PF, Offiah A, Tassy O, Pourquié O, Kusumi K, Dunwoodie S. Abnormal vertebral segmentation and the notch signaling pathway in man. Dev Dyn 2007;236:1456–1474. [PubMed: 17497699]

Wilkinson, DG. In situ hybridisation, a practical approach. Oxford University Press; Oxford: 1992. Whole mount in situ hybridisation of vertebrate embryos; p. 75-83.

William DA, et al. Identification of oscillatory genes in somitogenesis from functional genomic analysis of a human mesenchymal stem cell model. Dev Biol 2007;305:172–186. [PubMed: 17362910]

Zhang N, Gridley T. Defects in somite formation in lunatic fringe-deficient mice. Nature 1998;394:374–377. [PubMed: 9690472]

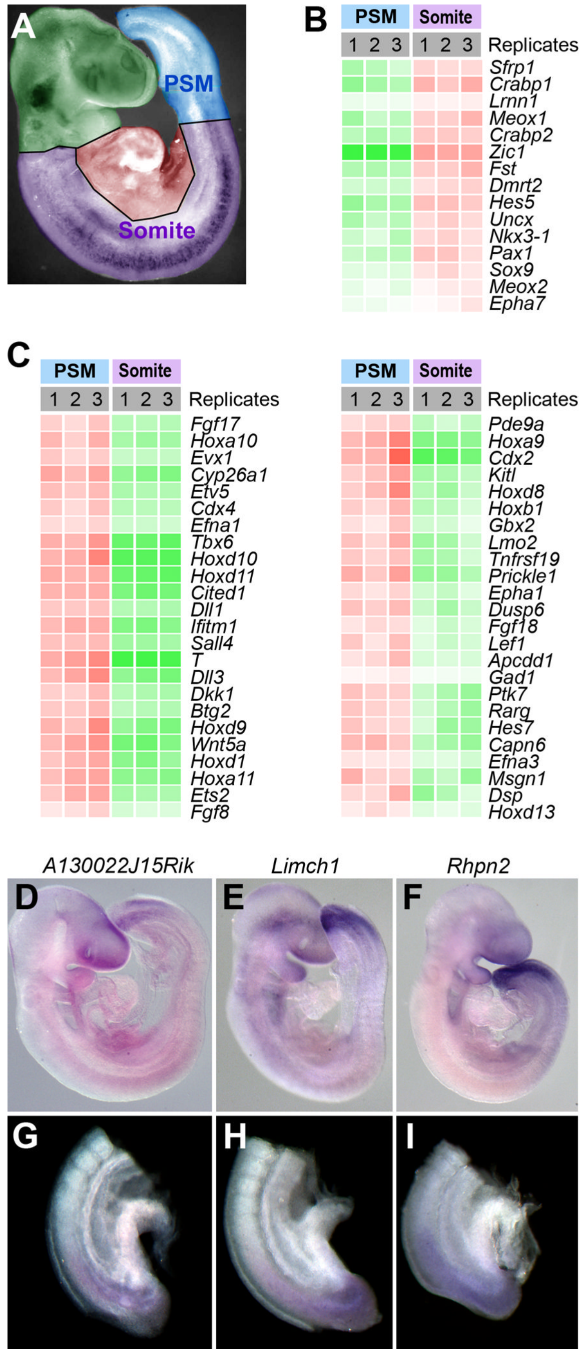

Figure 1.

Identification of novel genes expressed in presomitic mesoderm by microarray analysis of 9.5 dpc embryos. (A) Tissues from presomitic mesoderm and somites from ten 9.5 dpc embryos were pooled into each of three biological replicates per tissue. Total RNA extracted from each pool was analyzed using Affymetrix MOE430A arrays with a single round of target preparation. Genes are shown in order of gene-tree clustering. We identified 66 genes that were more than 2-fold increased in expression in somite level tissue compared to PSM (Supplemental Table S1), with 15 genes with reported expression in paraxial mesoderm (B), 48 genes reported in other tissues, and 3 genes uncharacterized (Table 1). We identified 87 genes that were more than 2-fold increased expression in PSM compared to somites

(Supplemental Table S2), with 48 genes with reported expression in paraxial mesoderm (C), 31 genes reported in other tissues, and 8 genes not previously described (Table 1). Analysis of these 8 genes identified three, *A130022J15Rik*, *Limch1*, and *Rphn2* that were highly expressed in the caudal PSM (D-I).

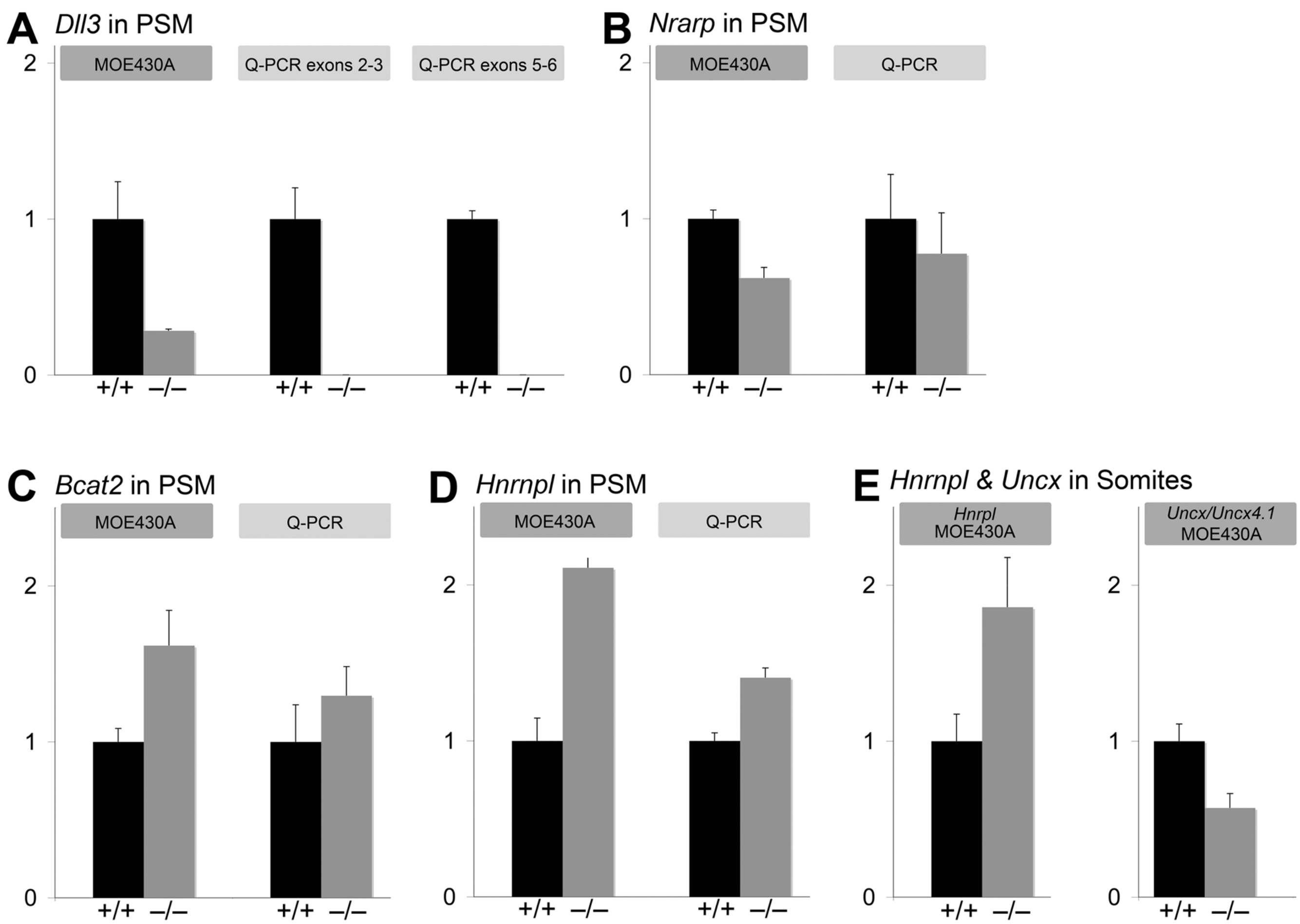

Figure 2.

Identification of genes in the paraxial mesoderm whose expression is disrupted by *Dll3* mutation. Tissues from *Dll3* mutant and wild type embryos at 9.5 dpc were microdissected into presomitic mesoderm and somite level tissues. Tissues from ten embryos were pooled into each biological replicate, with three replicates for each genotype, and analyzed on Affymetrix MOE430A arrays. Statistical analysis was carried out using a t-Test (two sample assuming unequal variance) and revealed all differences to be significant on a two-tailed test for initial microarray identification and at least on a one-tailed test for validation by Q-PCR. Two tailed p values are given, except as noted. In the PSM at a 1.5 fold threshold, we only identified 2 genes with decreased expression, *Dll3* (A; p<0.035) and *Nrarp* (B; p<0.001). We observed two genes with increased expression, *Bcat2* (C; p<0.021) and *Hnrnpl* (D; p<0.001). We observed by Q-PCR that *Dll3* transcripts were absent in *Dll3*$^{neo/neo}$ embryos both assayed before (*Dll3* exons 2–3; p<10^{-8}) and after (*Dll3* exons 5–6; p<10^{-6}) the neo-induced mutation, suggesting nonsense-mediated decay of the transcript from the targeted allele. *Nrarp* displayed decreased expression the *Dll3* homozygous mutant PSM (B; one tailed test p<0.032), and *Bcat2* (C; p<0.025) and *Hnrnpl* (D; p<0.001) displayed increased expression in *Dll3* homozygous mutant PSM. In somite tissue with a 1.5 fold threshold, we identified that *Uncx* displayed decreased expression (E right panel; p<0.006) and *Hnrnpl* was increased in expression (E left panel; p<0.026).

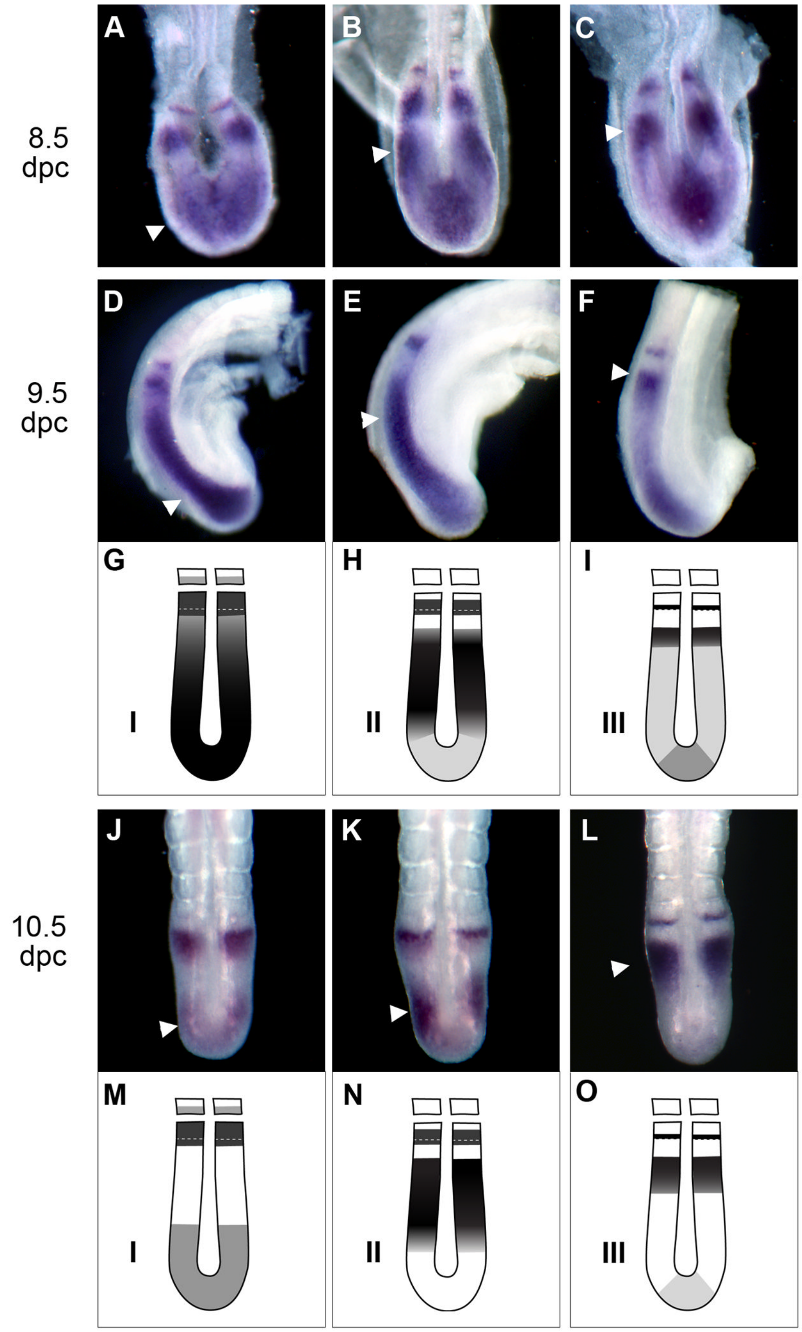

Figure 3.

Nrarp displays cycling expression in the presomitic mesoderm with distinct patterns at 8.5, 9.5, and 10.5 dpc. Embryos at 8.5 dpc (n=15; A–C; dorsal view), 9.5 dpc (n=50; D–F; lateral view), and 10.5 dpc (n=32; J–L; dorsal view) are shown in order corresponding to phases I–III (diagrammed in G–I for 9.5 dpc, M–O for 10.5 dpc), as defined previously for cycling genes (Pourquié and Tam, 2001). Regions of peak *Nrarp* expression are indicated (arrowheads). Rostral bands of *Nrarp* expression display anterograde shifts and contraction at 8.5–10.5 dpc, as characteristic of cycling genes. *Nrarp* expression in the caudal PSM extends over a larger proportion of the PSM at 8.5 and 9.5 dpc compared to 10.5 dpc. However, within this larger region in the PSM, the area of highest expression is observed to display anterograde shifts.

Tailbud expression of *Nrarp* decreases from phases I to II (G, H) and returns by phase III (I). *Nrarp* more clearly shows cycling expression at 10.5 dpc (arrowheads) with periodically decreased expression in the tailbud between phases II and III (K, L and N, O).

Figure 4.

Nrarp cycling expression displays a 2 hour periodicity. 9.5 dpc Mouse embryos were bisected, with left halves cultured for 15 minutes and fixed, and right halves cultured for an additional 1 hour (A, n=8), 2 hours (B, n=7), or 3 hours (C, n=7) prior to fixation. Embryo culture resulted in some shrinkage of tissue; therefore, the halves are aligned with the caudal border of the forming somite S0 (arrowhead). At a 1 hour time difference, anterograde shifts of *Nrarp* caudal expression in the PSM were observed (A). At a 2 hour time difference, cultured halves displayed similar expression patterns of *Nrarp*, as shown in (B). At 3 hour time differences, cultured halves again differed in *Nrarp* caudal expression (C). The observation that cultured halves were in the same phase at 2 hours, and out of phase at 1 and 3 hours, is consistent with the 2 hour periodicity of cycling genes during mouse somitogenesis.

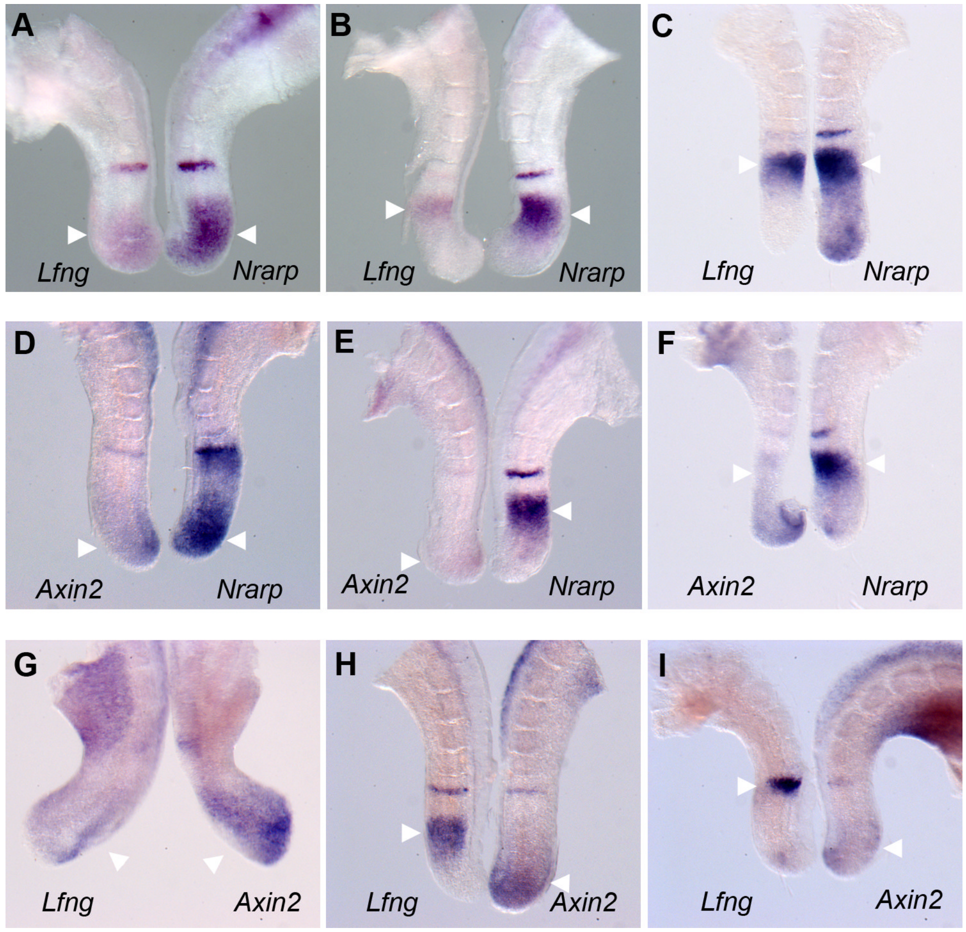

Figure 5.

Nrarp cycling expression is in phase with *Lfng* and out of phase with *Axin2* at 10.5 dpc. Mouse 10.5 dpc embryos were bisected and halves were analyzed by *in situ* hybridization (A–I). *Nrarp* expression was compared to *Lfng* (n=12; A–C) and the wnt pathway cycling gene *Axin2* (n=12; D–F); and *Lfng* and *Axin2* were compared to each other (n=18; G–I). Areas of peak expression are indicated (arrowheads). The caudal to rostral shifts in *Nrarp* expression corresponded to equivalent phases for *Lfng* (A–C). Neither the expression of *Nrarp* nor *Lfng* corresponded with cycling expression phases of *Axin2* (E, F and H, I, respectively). However, the cycling expression of *Axin2* at 10.5 dpc is less notable than at 9.5 dpc (Supplemental Fig. S2). All half embryos are aligned at S0 and oriented with rostral at the top.

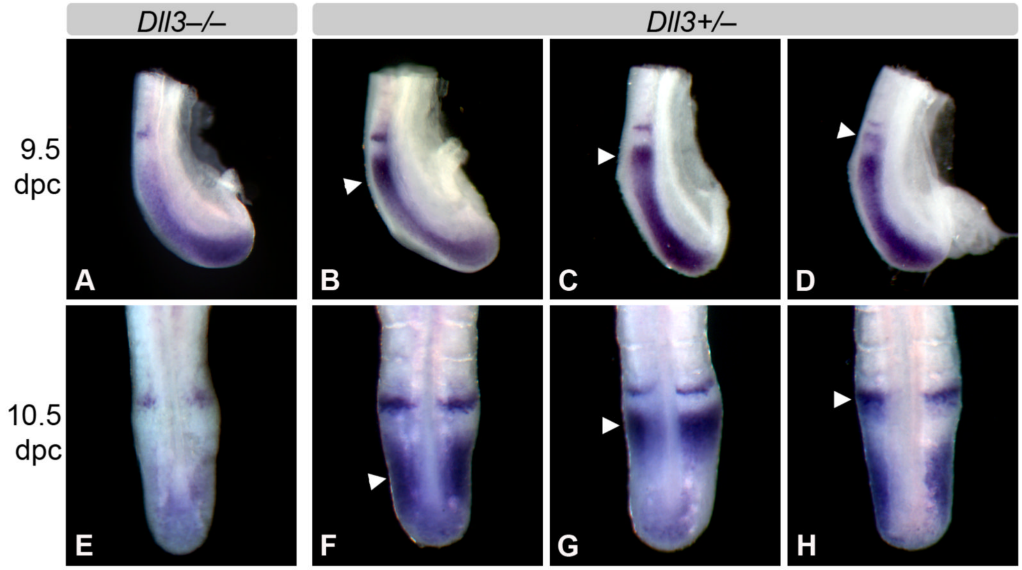

Figure 6.

Nrarp displays decreased expression and does not cycle in *Dll3* mutants. *Nrarp* expression was analyzed by *in situ* hybridization of 9.5 dpc stage *Dll3*$^{neo/neo}$ mutant (n=5; A), *Dll3*$^{neo/+}$ heterozygous (n=7; B), and *Dll3*$^{+/+}$ control (n=8; data not shown) embryos. *Nrarp* expression in the rostral PSM is strongly decreased in *Dll3*$^{neo/neo}$ 9.5 dpc embryos, and cycling expression was not observed. This observation was confirmed in 10.5 dpc stage *Dll3*$^{neo/neo}$ mutant (n=3; E), *Dll3*$^{neo/+}$ heterozygous (n=4; F–H), and *Dll3*$^{+/+}$ control (n=4; data not shown). Both *Dll3* heterozygous and wild-type embryos displayed cycling expression at 9.5 and 10.5 dpc (B–D, F–H, and data not shown).

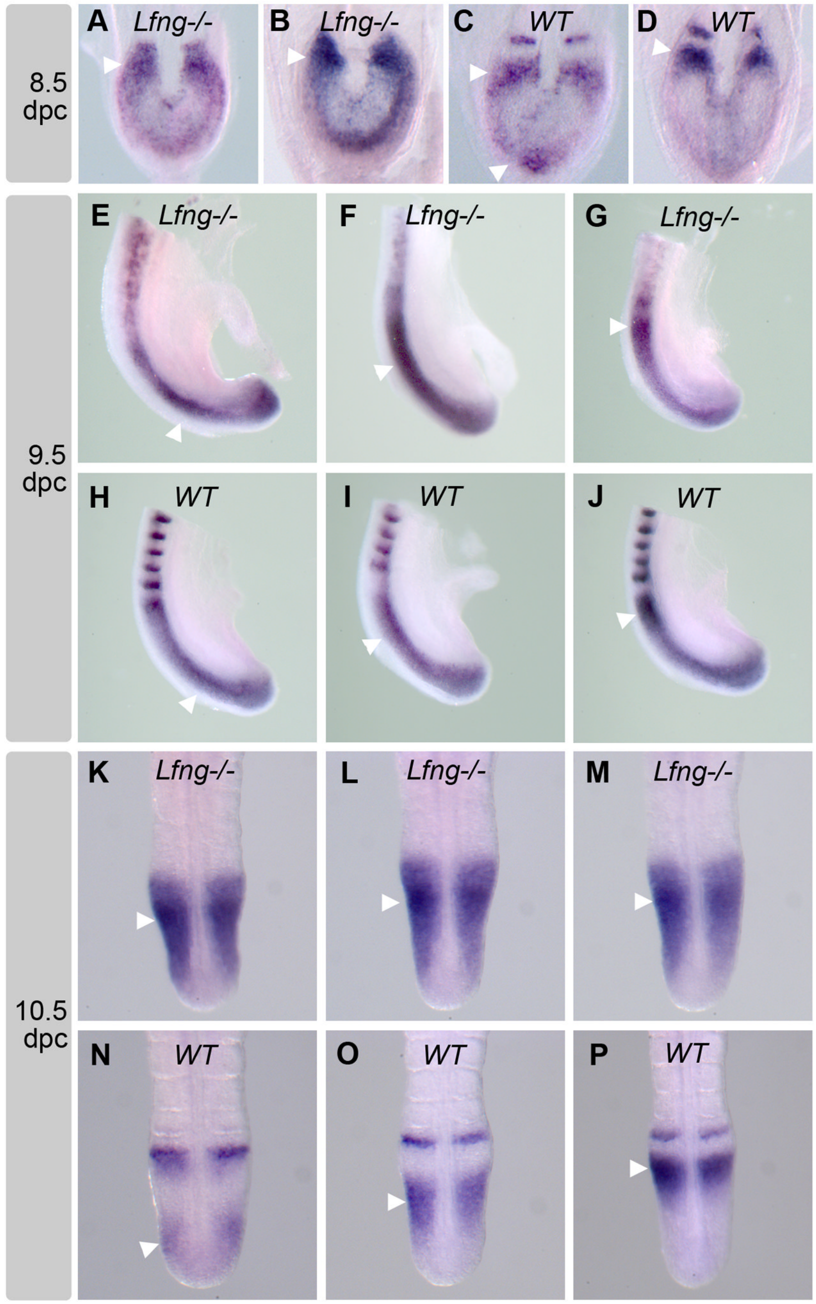

Figure 7.

Nrarp displays cycling expression in the presomitic mesoderm of *Lfng* mutant embryos. *Nrarp* expression was analyzed by *in situ* hybridization at 8.5, 9.5, and 10.5 dpc stages for $Lfng^{tm1Rjo/tm1Rjo}$ mutants (8.5 dpc, n=4; 9.5 dpc, n=5; 10.5 dpc, n=6) and wild-type controls (8.5 dpc, n=5; 9.5 dpc, n=5; 10.5 dpc, n=5). *Uncx*/*Uncx4.*1, which is expressed only in the caudal somites, was also added as a probe to hybridizations of the 9.5 dpc embryos in order highlight disruptions in segmentation in mutant embryos (E–G). Peak areas of *Nrarp* expression are indicated by arrowheads. In *Lfng* mutant embryos, *Nrarp* expression does not appear to be dynamic at 8.5 dpc (A, B) but clearly displays cycling expression at 9.5 dpc (E–G). In *Lfng* mutant embryos at 10.5 dpc, there was a subtle anterograde shift in peak *Nrarp*

NIH-PA Author Manuscript

NIH-PA Author Manuscript

expression and decreased expression in the caudal PSM in phase III (K–M), suggesting dynamic expression. *Lfng*$^{+/+}$ 10.5 dpc embryos demonstrate caudal-to-rostral shifts typical of oscillatory genes (N–P).

NIH-PA Author Manuscript

NIH-PA Author Manuscript

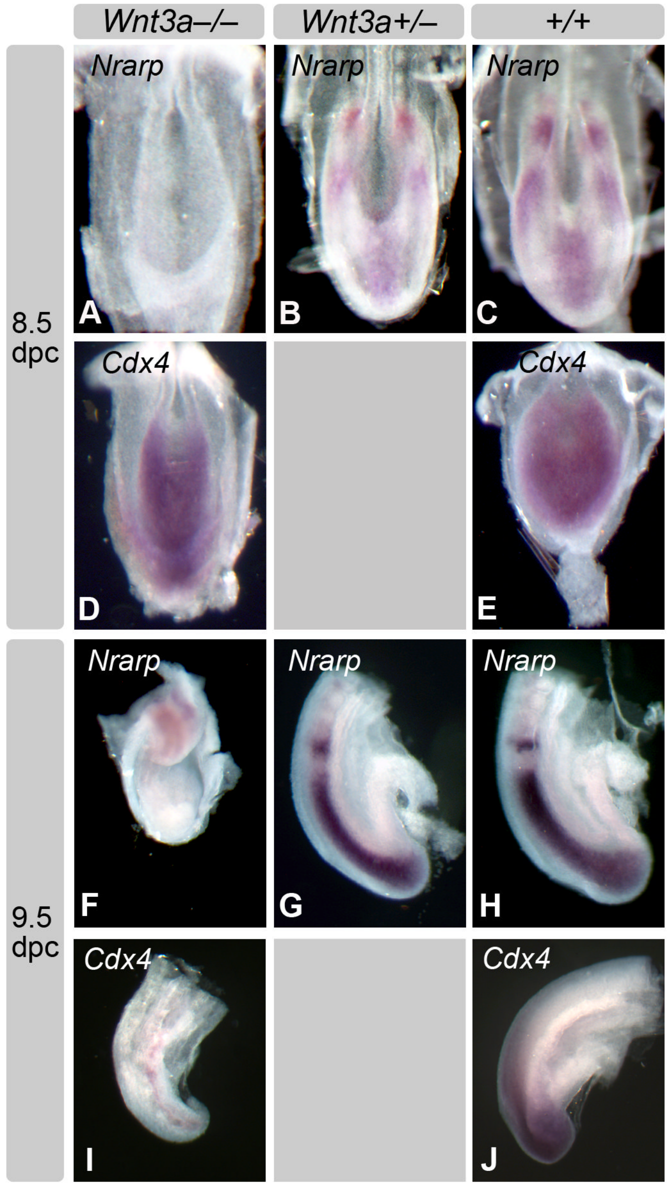

Figure 8.

Nrarp is not expressed in the PSM of *Wnt3a* homozygous mutants at 8.5 and 9.5 dpc. At 8.5 dpc, *Wnt3a* $^{tm1Amc/tm1Amc}$ (n=6; A), *Wnt3a*$^{tm1Amc/+}$ (n=5; B), and *Wnt3a*$^{+/+}$ (n=5; C) were analyzed by *in situ* hybridization with *Nrarp* probe. *Nrarp* expression was not observed in mutant embryos, which contained presomitic mesoderm as confirmed by hybridization with *Cdx4* probe (D, E). At 9.5 dpc, *Wnt3a* $^{tm1Amc/tm1Amc}$ (n=9; F), *Wnt3a*$^{tm1Amc/+}$ (n=10; G), and *Wnt3a*$^{+/+}$ (n=10; H) embryos were analyzed by *in situ* hybridization with *Nrarp* probe, which was not expressed in *Wnt3a* $^{tm1Amc/tm1Amc}$ mutants. Panels F–H show approximately equivalent tissues that are caudal to somite 3. At 9.5 dpc, *Wnt3a* $^{tm1Amc/tm1Amc}$ mutants had greatly reduced amounts of presomitic mesoderm compared to *Wnt3a*$^{+/+}$, as demonstrated by *in situ* hybridization with *Cdx4* probe (I, J).

Table 1

Expression of previously uncharacterized genes identified by microarray analysis of 9.5 dpc embryonic paraxial mesoderm.

Gene	Fold Change	Gene Description	Expression (9.5 dpc)
Genes enriched in somite level tissues			
Elav14	2.4	embryonic lethal abnormal vision-like 4	No expression detected
Itih5	2.6	inter-alpha (globulin) inhibitor H5	No expression detected
Pkdcc	4.8	protein kinase domain containing, cytoplasmic	Trunk mesenchyme, ventral somites (Fig. S1)
Genes enriched in PSM level tissues			
2610528A11Rik	7.4	RIKEN 2610528A11 gene	Caudal endoderm (Fig. S1)
A130022J15Rik	2.1	RIKEN A130022J15 gene	Caudal PSM (Fig. 1)
Arhgap24	3.1	Rho GTPase activating protein 24	Neural tube
Gzmk	2.1	granzyme K	No expression detected
Hsd17b11	2.4	hydroxysteroid 17-beta dehydrogenase 11	No expression detected
Limch1	2.3	LIM & calponin homology domains 1	Caudal PSM (Fig. 1)
Mpzl2	2.6	myelin protein zero-like 2	No expression detected
Rhpn2	2.8	rhophilin 2	Caudal PSM (Fig. 1)

NIH-PA Author Manuscript
NIH-PA Author Manuscript

Table 2

Distribution of patterns of *Nrarp*, *Lfng*, and *Axin2* gene expression between cycling phases I, II, and III

Gene	Embryo age	Phase I	Phase II	Phase III	p value (deviation from expected)
Lfng	9.5 dpc	38% (18/47)	26% (12/47)	36% (17/47)	p<0.517
Axin2	9.5 dpc	22% (10/45)	33% (15/45)	44% (20/45)	p<0.189
Nrarp	9.5 dpc	30% (12/40)	60% (24/40)	10% (4/40)	p<0.0005
Nrarp	10.5 dpc	37% (10/27)	52% (14/27)	11% (3/27)	p<0.0319

* *Lfng* and *Axin2* phases were determined as described in Aulehla et al., 2003. *Nrarp* phases were determined as described in Fig. 3. Percentages may not total 100% due to rounding.